

Exchange Frequencies in the 2d Wigner crystal

B. Bernu¹, Ladir Cândido² and D. M. Ceperley²

¹*Laboratoire de Physique Théorique des Liquides, UMR 7600 of CNRS, Université P. et M. Curie, boîte 121, 4 Place Jussieu, 75252 Paris, France*

²*Dept. of Physics and NCSA University of Illinois at Urbana-Champaign, Urbana, IL 61801*

Using Path Integral Monte Carlo we have calculated exchange frequencies as electrons undergo ring exchanges in a “clean” 2d Wigner crystal as a function of density. The results show agreement with WKB calculations at very low density, but show a more rapid increase with density near melting. Remarkably, the exchange Hamiltonian closely resembles the measured exchanges in 2d ³He. Using the resulting multi-spin exchange model we find the spin Hamiltonian for $r_s \leq 175 \pm 10$ is a frustrated antiferromagnetic; its likely ground state is a spin liquid. For lower density the ground state will be ferromagnetic.

PACS Numbers: 73.20Dx, 75.10-b, 67.8Jd

The uniform system of electrons is one of the basic models of condensed matter physics. In this paper, we report on the first exact calculations of the spin Hamiltonian in the low density 2 dimensional Wigner crystal (2dWC) near melting. This system is realized experimentally with electrons confined at an semiconductor MOS-FET's and heterostructures [1], and for electrons on the surface of liquid helium [2].

A homogeneous charged system is characterized by two parameters: the density given in terms of $r_s = a/a_0 = (m^*/m\epsilon)(\pi a_0^2 \rho)^{-1/2}$ and the energy in effective Rydbergs $Ry^* = (m^*/m_e \epsilon^2) Ry$ where m^* is the effective mass and ϵ the dielectric constant. Figure 1 summarizes the 2d phase diagram. At low density (large r_s) the potential energy dominates over the kinetic energy and the system forms a perfect triangular lattice, the Wigner crystal [3]. Tanatar and Ceperley [4] determined that melting at zero temperature occurs at $r_s \simeq 37 \pm 5$. Recent calculations [5] have shown that the low temperature phase is free of point defects for densities with $r_s \geq 50$ but defects may be present very near melting. At densities for $r_s \geq 100$ the melting is classical, and occurs for temperatures $T_{melt} = 2Ry/(\Gamma_c r_s)$ where $\Gamma_c \approx 137$ [6].

We determine the spin-spin interaction in the Wigner crystal, using Thouless' [8] theory of exchange. According to this theory, in the absence of point defects, at low temperatures the spins will be governed by a Hamiltonian of the form:

$$\mathcal{H}_{spin} = - \sum_P (-1)^P J_P \hat{P}_{spin} \quad (1)$$

where the sum is over all cyclic (ring) exchanges described by a cyclic permutation P , J_P is its exchange frequency and \hat{P}_{spin} is the corresponding spin exchange operator. Path Integral Monte Carlo (PIMC) as suggested by Thouless [8] and Roger [9] has proved to be the only reliable way to calculate these parameters. The theory and computational method have been tested thoroughly on the magnetic properties of bulk helium obtaining excellent agreement with measured properties [10]. Rather

surprisingly, it has been found [11] that in both 2d and 3d solid ³He, exchanges of 2, 3 and 4 particles have roughly the same order of magnitude and must all be taken into account. This is known as the multiple spin exchange model(MSE).

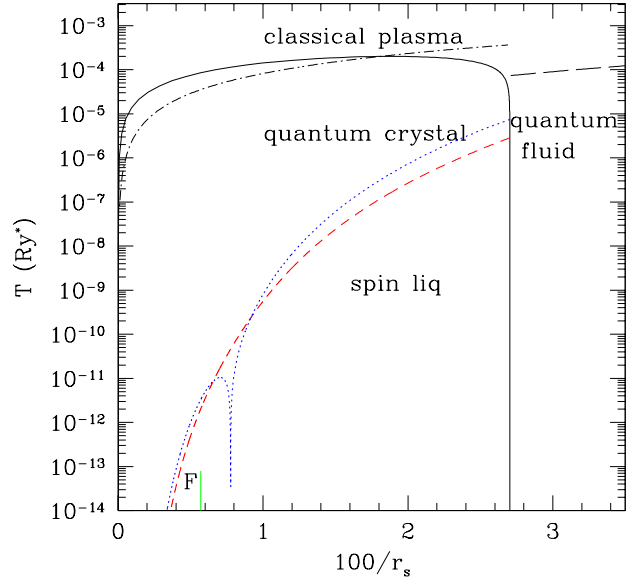


FIG. 1. Phase diagram. The estimated melting line is based on Lindemann's criteria [7]. The long-dashed line represents the Debye temperature. The dotted line is θ , the short dashed line is J_c . The vertical line is the estimated zero temperature ferromagnetic (F) transition.

A WKB calculation of the exchange frequencies in the 2dWC by Roger [9] predicted that the three electron J_3 nearest neighbor exchange would dominate, leading to a ferromagnetic(F) ground state. It has been recently pointed out [12] that if the 2dWC can be stabilized by

disorder to higher densities, a transition to an antiferromagnetic(AF) phase will occur. Although the $1/r$ interaction is characterized as ‘soft’, in the 2dWC the two particle pair correlation function for the electron system is quite similar to that of solid ^3He supporting the idea that multiple exchanges could be important in the 2dWC near melting.

The method of determining the exchange frequency in quantum crystals has been given earlier [10,13,14]. One computes the free energy necessary to make an exchange beginning with one arrangement of particles to lattice sites Z and ending on a permuted arrangement PZ :

$$F_P(\beta) = Q(P, \beta)/Q(I, \beta) = \tanh(J_P(\beta - \beta_0)). \quad (2)$$

Here $Q(P, \beta)$ is the partition function corresponding to an exchange P at a temperature $1/\beta$. I is the identity permutation. Note that these paths are of “distinguishable” particles since Fermi statistics are implemented through the spin Hamiltonian in Eq. (1). We determine the function $F_P(\beta)$ using a method which directly calculates free energy differences and thereby determines J_P and β_0 . The only new feature with respect to the ^3He calculations is the method of treating the long-range potential. We use the standard Ewald breakup [9] and treat the short-range part using the exact pair action [10] and the long-range k-space term using the primitive approximation. We used a hexagonal unit cell with periodic boundary conditions, most calculations containing 36 electrons. Checks with up to 144 electrons did not change the results within the statistical errors. The number of particles is not as important in the 2dWC as in solid ^3He because the $1/r$ interaction suppresses the long wavelength charge fluctuations.

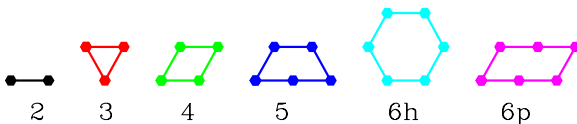


FIG. 2. Considered exchanges.

We performed calculations for the densities $r_s = \{45, 50, 60, 75, 100, 140, 200\}$. We found accurate results using a “time-step” for the discretized imaginary time path integrals of $\tau \leq 0.3r_s^{3/2}$ and extrapolated to the $\tau = 0$ limit using $J_p(\tau) = J_p(0) + J'_p\tau^3$. The inverse temperature β in Eq. (2) must be larger than the values determined by melting and twice the exchange “time” $\beta_0 \sim 5r_s^{3/2}$. We have determined the exchange frequencies with an accuracy between 1.5% and 6% independent of their magnitude or the number of exchanging electrons though the computer time increases with the number of exchanging electrons. Breakdown of Thouless’ theory caused by many states contributing to the ratio of parti-

tion functions would be signaled by $F_P(\beta)$ not described by Eq. (2). Except for $r_s < 50$ where our calculations are too unstable to make definite predictions, we observed no problems of convergence.

Figure 2 shows the ring exchanges considered here. Except near melting these exchanges give rise to most of the thermodynamic properties. Note that we consider the 6-particle parallelogram (6p) exchange, which is not taken into account in solid ^3He . We have also calculated several 2-5 particle exchanges having next-nearest neighbor exchanges and all possible 6 particle nearest-neighbor exchanges for $50 \leq r_s \leq 75$, but because their magnitudes are much smaller, we do not report those results.

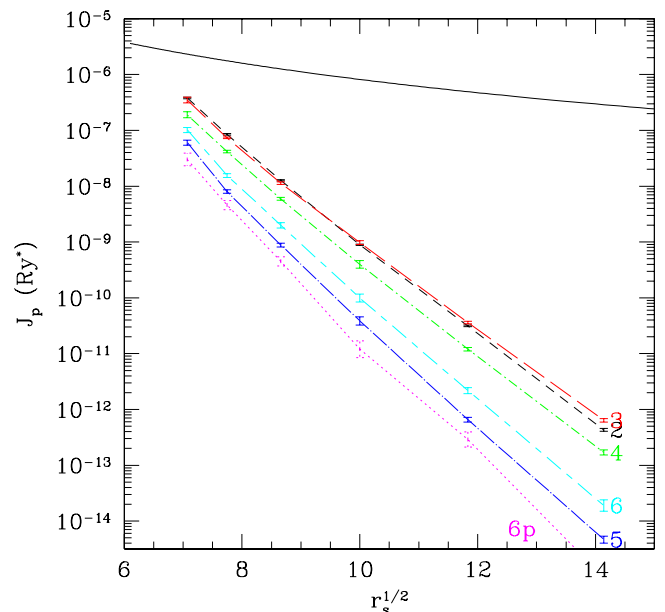


FIG. 3. Exchange frequencies versus $r_s^{1/2}$. The solid line is 10^{-3} of the kinetic energy.

Our calculated exchange frequencies vary rapidly with density as shown in fig. (3). One can see that they are much less than the zero point energy of the electrons, thus justifying the use of Thouless’ theory. The WKB method [11] where one approximates the Path Integral in Eq. (2) by the single most probable path, explains most of this density dependence. In the 2dWC, the WKB expression for the exchange frequency [9,12] is:

$$J_P = A_P(r_s) b_P^{1/2} r_s^{-5/4} e^{-b_P r_s^{1/2}}. \quad (3)$$

Here $b_P r_s^{1/2}$ is the minimum value of the action integral along the path connecting PZ with Z . The 3 particle exchange exponent is the smallest indicating that as $r_s \rightarrow \infty$, J_3 will dominate and the system will have a

ferromagnetic ground state. However, note that in fig. (3) $J_2 > J_3$ for $r_s \leq 90$. We observe a more rapid increase in all the exchange frequencies than predicted by Eq. (3) for $r_s < 100$ caused by non-linear fluctuations about the classical path. Near melting the spread in exchange frequencies is much less than in the low density limit.

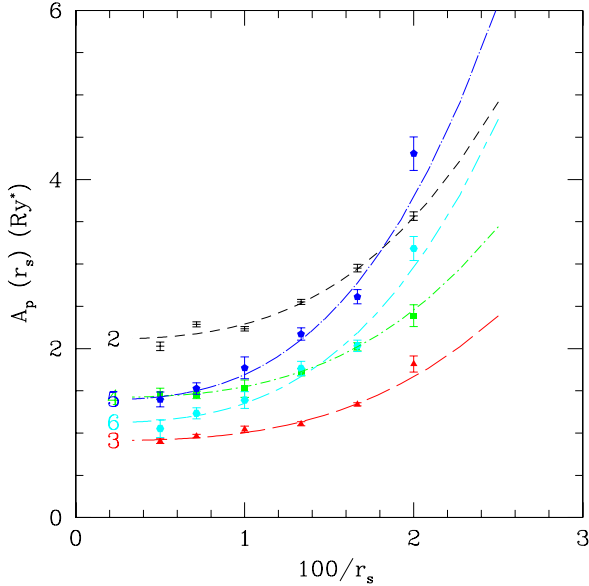


FIG. 4. The prefactor of the exchange frequencies, A_P , see Eq. (3) versus density. All prefactors go to a constant for $r_s > 100$ indicating that exchange frequencies are dominated by a single path (WKB limit). The curves are fits as described in the text.

Figure (4) shows density dependence of the prefactor, A_P . The prefactors are larger than unity as expected [12] (our definition of A_P differs from ref. [12] by a factor of $1.63/\sqrt{2\pi}$). We observe that the prefactor is roughly constant for $r_s > 100$ but rises rapidly as the system approaches the melting density. We are unaware of any work that definitively establishes the form of the correction to the WKB formula. A good fit was obtained with the function $A_P(r_s) = A_P(0)(1 + (r_P/r_s)^3)$ to determine b_P , $A_P(0)$ and r_P . The exponents are close to the WKB values, only differing significantly for the 2-particle exchange.

The prefactor for J_2 is twice as large as the other exchanges. One might think that since one cannot observe the difference in pair exchanges in the initial and final spins, the sense of the exchange would not matter. Our results show that the 2 orientations of 2 particle exchange, clockwise and counter-clockwise, should

be counted separately. A recent calculation [15] directly evaluates J_2 in the high density regime, $5 \leq r_s \leq 45$, by numerically solving for the difference between the even and odd parity 2-electron energies. In those calculations, the spectator electrons were fixed at their lattice sites and the 2 exchanging electrons had vanishing wavefunctions outside a rectangle centered around the exchange. At $r_s = 45$ a direct comparison shows their result is 2.3 times larger than that obtained with PIMC. This result is expected because of the additional localization caused by the spectator electrons fluctuating into the exchanging region.

Having determined the exchange frequency, one is left with the spin Hamiltonian of Eq. (1). This is a non-trivial many-body problem which we will not discuss in detail here. For spin 1/2 systems, J_2 and J_3 contribute only with a nearest neighbor Heisenberg term: $J_2^{\text{eff}} = J_2 - 2J_3$. This term is negative (ferromagnetic) but approaches zero near melting. For convenience we use J_4 as a reference to fix the overall scale of the magnetic energy. Neglecting J_{6p} , the Hamiltonian has 3 remaining parameters J_2^{eff}/J_4 , J_5/J_4 and J_{6h}/J_4 . The dependence of these ratios on density is shown in fig. (5).

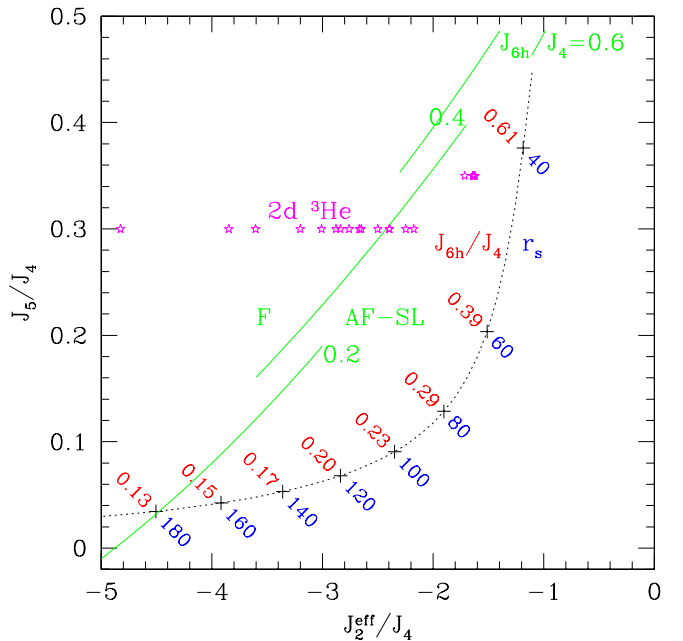


FIG. 5. Spin Phase diagram as a function of exchange ratios. The dotted line is the flow of spin Hamiltonian space versus r_s (lower numbers); also shown are estimated values of J_{6h}/J_4 (upper numbers). The solid lines are the limit of the ferromagnetic phase according to ED [17] at $J_{6h}/J_4 = \{0.2, 0.4, 0.6\}$. The 2dWC crosses into the F region for $r_s \approx 175$. The (*) are empirical estimates of the spin Hamiltonian of 2d ^3He at several densities [19].

High temperature series expansions [16] determine the the specific heat C_V and magnetic susceptibility χ_0/χ for temperatures $k_B T \gg J_P$. The susceptibility is given by: $\chi_0/\chi = T - \theta + B/T \dots$ and the specific heat $C_V/Nk_B = (3J_c/2T)^2 + \dots$ where the Curie-Weiss constant is given by $\theta = -3(J_2^{\text{eff}} + 3J_4 - 5J_5 + 5/8J_{6h} + 15/4J_{6p})$ with a quadratic expression of the J 's for J_c . These two constants which set the scale of the temperature where exchange is important are shown as a dotted and dashed lines on fig. (1). Both θ and J_c decrease very rapidly at low density showing that experiments must be done at $r_s \leq 100$ if spin effects are to be at a reasonable temperature, e.g. $T_c > 0.1mK$ (assuming $\epsilon = m^* = 1$). Note that θ changes from positive to negative at $r_s \approx 130$.

The zero temperature state can be studied by exact diagonalization (ED) of an N site system. (The present limitation is $N \lesssim 36$.) Here we focus on the zero temperature transition from a ferromagnetic to an antiferromagnetic state. An estimate [17] of the critical transition parameters is shown on fig.(5). The ferromagnetic phase is obtained only at very low density: we estimate the the F-AF transition for the 2dWC will occur at $r_s = 175 \pm 10$. (Note that this estimate does not include the effect of J_{6p} ; this will increase the stability of the antiferromagnetic region to roughly $r_s = 200$.)

At higher density, the frustration between large cycle exchanges (4-6 body loops) results in a disordered spin state. For example, the point ($J_2^{\text{eff}}/J_4 = -2$, $J_5 = 0$, $J_{6h} = 0$), close to the parameters at $r_s = 100$, is a spin liquid with a gap to all excitations [17]: The spin liquid properties can be understood from a resonance valance bond model with ordering into spin-1 diamond plaquettes. The breakup of the plaquettes is responsible for a low temperature peak on the specific heat. A second high temperature peak develops at a temperature $T \sim J_c$, shown as a dotted line on fig. (1).

We find that at higher densities ($r_s < 100$), the trajectory of the MSE models parallels the F-AF phase line, with the possibility of a re-entrant ferromagnetic phase for $r_s < 40$. Note that QMC calculations [18] of the normal fermi liquid at $r_s = 30$ show that the ferromagnetic phase has a slightly lower energy than the unpolarized phase. Hence both the high density 2dWC and the low density electron fluid are characterized by a spin Hamiltonian which is nearly ferromagnetic.

We note a remarkable similarity between the exchange parameters of the 2dWC to those extrapolated from mea-

surements of the second layer of ^3He absorbed on grafoil [19] as shown in fig. (5). The existence of these two related spin systems should allow a fuller understanding of this remarkable spin liquid. Such an equivalence could arise from an underlying virtual vacancy-interstitial (VI) mechanism [11] giving rise to ring exchanges. In this model the prefactor of the exchange is controlled by the rate of VI formation (non-universal) but the ratios of the various ring exchanges arises from geometry of the triangular lattice and from the attraction of point defects (universal). We have recently determined [5] that the VI formation energy vanishes at melting in the 2dWC. This is consistent with the fact that the various J_P increase rapidly near melting.

In summary, we find that the magnetic interactions are characterized by a frustrated spin order. Application of a magnetic field [20] transforms the exchange frequencies to $J_P e^{2\pi i e B_{\perp} a_P / h}$ where a_P is the area of the exchange (see table I) and B_{\perp} the magnetic field. Experiments with magnetic fields will allow exploration of this Aharonov-Bohm effect and thereby provide direct information on ring exchanges.

The semiconductor realizations of the 2dWC have significant disorder which can stabilize localized electronic states at higher densities than in the clean system [21]. One can also stabilize the Wigner crystal at higher densities using bilayers [22]. Exchange frequencies in those systems including effects of layer thickness and the exchange properties of point defects could be calculated with the present method.

This research was funded by NSF DMR 98-02373, the CNRS-University of Illinois exchange agreement, support by Fundação de Amparo à Pesquisa do Estado de São Paulo (FAPESP) and the Dept. of Physics at the University of Illinois. We used the computational facilities at the NCSA.

P	b_P	$A_P(0)$	r_P	a_P
2	1.612	2.11	44	
3	1.525	0.91	47	2.07(1)
4	1.656	1.42	45	3.07(2)
5	1.912	1.39	60	4.11(2)
6h	1.790	1.12	59	7.04(3)
6p	2.136	6.24	38	5.09(2)

TABLE I. Fits for the exchange frequencies. The path area, a_P , was calculated at $r_s = 60$ and it is in units of triangle areas.

[1] J. Yoon *et al.*, Phys. Rev. Letts. **82**, 1744 (1999).
[2] C. C. Grimes and G. Adams, Phys. Rev. Lett. **42**, 795 (1979).
[3] X. Zhu and S. G. Louie, Phys. Rev. B **52**, 5863 (1995).

[4] B. Tanatar and D. M. Ceperley, Phys. Rev. B **39**, 5005 (1989).
[5] L. Cândido, P. Phillips and D. M. Ceperley, cond-mat/0002366.
[6] K. Strandburg, Rev. Mod. Phys. **60**, 161 (1988).
[7] F. Douchin, L. Cândido and D. Ceperley, to be published.
[8] D. J. Thouless, Proc. Phys. London **86**, 893 (1965).
[9] M. Roger, Phys. Rev. B **30**, 6432 (1984).

- [10] D. M. Ceperley, Rev. Mod. Phys. **67**, 279 (1995).
- [11] M. Roger, J. H. Hetherington and J. M. Delrieu, Rev. Mod. Phys. **55**, 1 (1983).
- [12] S. Chakravarty, S. Kivelson, C. Nayak and K. Voelker, Phil. Mag. B **79**, 859 (1999).
- [13] D. M. Ceperley and G. Jacucci, Phys. Rev. Letts. **58**, 1648 (1987).
- [14] B. Bernu and D. Ceperley in *Quantum Monte Carlo Methods in Physics and Chemistry*, eds. M.P. Nightingale and C.J. Umrigar, Kluwer (1999).
- [15] V. V. Flambaum, I. V. Ponomarev and O. P. Sushkov, Phys. Rev. B **59**, 4163 (1999).
- [16] M. Roger, Phys. Rev. B **56**, R2928 (1997).
- [17] G. Misguich, B. Bernu, C. Lhuillier and C. Waldtmann, Phys. Rev. Letts. **81**, 1098 (1998); Phys. Rev. B **60**, 1064 (1999).
- [18] D. Varsano, S. Moroni and G. Senatore, cond-mat/0006397.
- [19] M. Roger, C. Bauerle, Yu. M. Bunke, A.-S. Chen and H. Godfrin, Phys. Rev. Letts. **80**, 1308 (1998).
- [20] T. Okamoto and S. Kawaji, Phys. Rev. B **57**, 9097 (1998).
- [21] S. T. Chui and B. Tanatar, Phys. Rev. Letts. **74**, 458 (1995).
- [22] F. Rapisarda and G. Senatore, Aust. J. Phys. **49**, 161 (1996); Int. J. Mod. Phys. B **13**, 479 (1999).